Acta Crystallographica Section D
Biological Crystallography
ISSN 0907-4449

Structure of apo, unactivated insulin-like growth factor-1 receptor kinase at 1.5 Å resolution

Sanjeev Munshi,* Dawn L. Hall, Maria Kornienko, Paul L. Darke and Lawrence C. Kuo

Department of Structural Biology, Merck Research Laboratories, West Point PA 19486, USA

Correspondence e-mail: sanjeev_munshi@merck.com

Received 19 May 2003
Accepted 11 July 2003

PDB Reference: IGFRK-0P, 1p4o, r1p4osf.

The crystal structure of the wild-type unactivated kinase domain (IGFRK-0P) of insulin-like growth factor-1 receptor has been reported previously at 2.7 Å resolution [Munshi *et al.* (2002), *J. Biol. Chem.* **277**, 38797–38802]. In order to obtain a high-resolution structure, a number of variants of IGFRK-0P were prepared and screened for crystallization. A double mutant with E1067A and E1069A substitutions within the kinase-insert region resulted in crystals that diffracted to 1.5 Å resolution. Overall, the structure of the mutant IGFRK-0P is similar to that of the wild-type IGFRK-0P structure, with the exception of the previously disordered kinase-insert region in the wild type having become fixed. In addition, amino-acid residues 947–952 at the N-terminus are well defined in the mutant structure. The monomeric protein structure is folded into two lobes connected by a hinge region, with the catalytic center situated at the interface of the two lobes. Two molecules of IGFRK-0P in the asymmetric unit are associated as a dimer and two different types of dimers with their ATP-binding clefts either facing towards or away from each other are observed. The current refined model consists of a dimer and 635 water molecules.

1. Introduction

A number of transmembrane receptor protein tyrosine kinases have been identified as critical components of cellular signaling processes. The insulin-like growth factor-1 receptor (IGF-1R), a member of the protein tyrosine kinase superfamily, has been suggested to play important roles in cell division, development and metabolism (Baserga *et al.*, 1994; LeRoith *et al.*, 1995). Upon binding of the growth factors IGF-1 and/or IGF-2, IGF-1R is activated. In the activated state, IGF-1R has been implicated to participate in oncogenesis and suppression of apoptosis (Baserga, 1999; Adams *et al.*, 2000). During activation, several specific tyrosine residues of IGF-1R are phosphorylated. Phosphorylation is essential not only for the catalytic activity of the kinase domain of IGF-1R but also for the recruitment of the downstream components of the signaling pathway. A number of cancer cell lines overexpress IGF-1R. Down regulation of IGF-1R expression leads to inhibition of tumorigenesis and elevates tumor-cell apoptosis (Bhatavdekar & Neema, 1994; Macaulay *et al.*, 1990; Resnicoff & Baserga, 1996; D'Ambrosio *et al.*, 1996; Prager *et al.*, 1994; Gansler & Garvin, 1989; Mercola & Cohen, 1995; Baserga *et al.*, 1997). Thus, inhibition of IGF-1R activity may serve as a therapeutic approach to develop anticancer drugs (Baserga, 1996). Inhibitors may be designed against the unactivated or activated IGF-1R kinase domain.

IGF-1R is a heterotetrameric molecule consisting of two pairs of polypeptides, the α- and β-chains, that are linked by disulfide bonds (Oh *et al.*, 1993; Yarden & Ulrich, 1988). The α-chains are extracellular and provide binding for growth factors, whereas the β-chains are composed of a short extracellular region, a transmembrane region, an intracellular tyrosine kinase domain and a C-terminal tail (Hubbard & Till, 2000). Structures of the first three domains of the extracellular region of IGF-1R (Garrett *et al.*, 1998) and the kinase domain in the tris-phosphorylated (Favelyukis *et al.*, 2001) and bis-phosphorylated (Pautsch *et al.*, 2001) forms are available. Recently, the crystal structure of the unphosphorylated apo form of this tyrosine kinase domain (IGFRK-0P) has been reported at 2.7 Å resolution (Munshi *et al.*, 2002), but a high-resolution structure of the unactivated enzyme is deemed necessary to guide inhibitor optimization. The poor reproducibility and low-diffraction resolution of the wild-type apo crystals of IGFK-0P has led to our search for better diffracting crystals.

Here, we report the crystal structure at 1.5 Å resolution of a 321-residue form of IGFRK-0P that contains two mutated surface residues (E1067A and E1069A). These mutations enable the preparation of reproducible and highly ordered single crystals of IGFRK-0P.

2. Materials and methods

2.1. Cloning, expression and purification

The IGF-1R kinase domain used in this study was comprised of 321 amino acids, from residue 944 to residue 1264, of the human receptor (numbering according to Ullrich *et al.*, 1986). Two variants of this protein with two residues mutated to alanine (K1025A/E1026A; E1067A/E1069A) and one variant with three residues mutated to alanine (K1237A/E1238A/E1239A) were constructed. The lysine and glutamate residues targeted for mutations were identified as prescribed by Longenecker *et al.* (2001). The mutant enzymes were expressed in insect cells and purified as described previously (Munshi *et al.*, 2002).

2.2. Crystallization of the double mutant of IGFRK-0P

Crystals of the mutant form of the 321-residue IGFRK-0P were obtained by vapor diffusion using sitting drops incubated at 277 K. The protein solution, buffered to pH 7.5, contained 12 mg ml^{-1} IGFRK-0P, 20 m*M* Tris–HCl and 5 m*M* dithiothreitol. Rod-shaped crystals were obtained using a reservoir solution containing 0.1 *M* Tris–HCl at pH 8.5, 8% PEG 8K, 0.1 *M* LiCl, 10% ethylene glycol and 10% glycerol. Protein and reservoir solutions were mixed in a 1:1(*v*/*v*) ratio.

2.3. Data collection

Crystals were harvested into a solution containing the reservoir solution plus 20% glycerol and soaked for 2 min prior to flash-cooling in liquid nitrogen. The crystals were transferred onto a goniostat, which was bathed in a liquid-nitrogen stream. X-ray diffraction data were recorded on an ADSC Quantum 4 detector at the ID17 beamline of IMCA at the Advanced Photon Source, Chicago. The IGFRK-0P crystals diffracted X-rays to 1.5 Å resolution. The crystals belonged to space group $P2_1$, with a unit-cell volume consistent with two kinase molecules per asymmetric unit. The solvent content of the crystals was 52% assuming a partial specific volume of 0.74 cm g^{-1}. The data were processed using *HKL*2000 (Otwinowski & Minor, 1997). Diffraction data and refinement statistics are presented in Table 1.

Table 1
Diffraction parameters and refinement statistics.

Values in parentheses are for the highest resolution shell.

Space group	$P2_1$, 2 mols in AU
Unit-cell parameters (Å, °)	a = 52.9, b = 85.56, c = 78.8, β = 99.10
Resolution (Å)	1.5 (1.55–1.50)
Observed reflections	1497973
Unique reflections	98666 (5844)
Completeness (%)	90 (53)
R_{sym} (%)	7.9 (36.8)
$\langle I/\sigma(I)\rangle$	19.1 (1.7)
Refinement statistics	
Resolution limits (Å)	6–1.5
Reflections used	89907
R factor (%)	20.9
R_{free} (%)	23.6 with 10% data used
No. of solvent molecules	635
R.m.s.d. bond length (Å)	0.005
R.m.s.d. bond angle (°)	1.22
Ramachandran plot statistics (%)	
Residues in most favored region	92.5
Residues in additional allowed region	7.5

2.4. Structure determination and refinement

The structure of the mutant IGFRK-0P was determined with the molecular-replacement method using the program *AMoRe* (Navaza, 1994; Collaborative Computational Project, Number 4, 1994). The structure of wild-type IGFRK-0P (Munshi *et al.*, 2002) was used as the initial phasing model. Initially, the N-terminal and C-terminal domains were independently refined as rigid domains. Rigid-body refinement was followed by simulated annealing and automatic solvent modeling using the program *CNX* (Brünger *et al.*, 1998; Molecular Simulations Inc., San Diego). Model building was performed using the X-BUILD option in the program *QUANTA* (Molecular Simulations Inc., San Diego). The conformation of the refined structure was evaluated with *PROCHECK* (Laskowski *et al.*, 1993).

3. Results and discussion

3.1. Crystals of the mutant apo IGFRK-0P

The 321-amino-acid construct used in the present studies covered a length of the IGF-1R receptor from residue 944 to residue 1264. The N-terminal amino-acid sequence began with ASVN... and the C-terminal sequence ended with ...EELD. All three mutant forms of the 321-residue IGFRK-0P were cloned, expressed, purified and screened for crystallization. However, only the variant with mutations

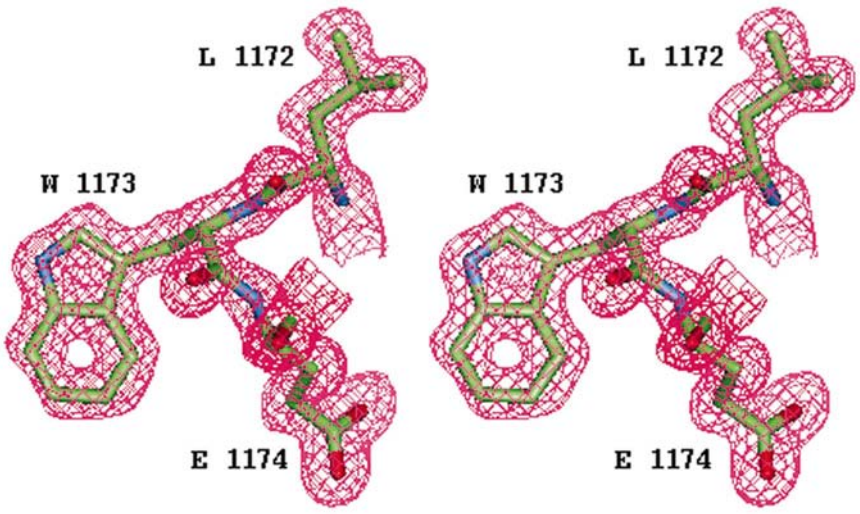

Figure 1
A region of the $2F_o - F_c$ map with residues 1172–1174 modeled in the density contoured at 1σ.

Figure 2
A ribbon representation of an IGFRK-0P monomer. The β-strands are colored cyan; the α-helices are colored lavender.

E1067A/E1069A yielded rod-shaped crystals within 4 d and diffracted to 1.5 Å resolution. In an enzymatic assay, this mutant of IGFRK-0P showed activity comparable to that of the wild type (data not shown), suggesting that the mutations in the kinase-insert region did not affect the overall folding of the enzyme.

3.2. Structure determination

Owing to the apparent similarities in the crystal packing between the wild type (space group $P2_1$; unit-cell parameters $a = 52.9$, $b = 78.1$, $c = 78.9$ Å, $\beta = 99.2^\circ$) and the mutant (see Table 1), the wild-type structure (Munshi *et al.*, 2002) was used as a search model. The most significant solutions of the rotation and translation functions led to a correlation coefficient and R factor of 0.54 and 36%, respectively.

After one round of conjugate-gradient minimization followed by simulated annealing, the $R_{\rm free}$ and R-factor values were lowered to 36.5 and 30.6%, respectively. Subsequent analysis of the electron-density maps, followed by model building and refinement, resulted in a model in which most of the side chains of the protein, including those in the kinase-insert region previously reported as disordered, were well defined. No efforts were made to impose twofold non-crystallographic symmetry constraints during refinement. Using all data in the resolution range 6–1.5 Å, the mutant IGFRK-0P structure was refined to a crystallographic R factor of 21% (Table 1). The refined model consisted of two molecules of the kinase and 635 water molecules.

Fig. 1 shows a region of the electron density covering residues 1172–1174 in one of the two molecules in the asymmetric unit. The two molecules are nearly identical in structure. The intermolecular interface within the asymmetric unit is conserved between the wild-type and mutant structures. In solution, IGFRK-0P is known to exist as a monomer.

3.3. Overall structure of IGFRK-0P

The overall structure of the mutant IGFRK-0P is similar to that of the wild-type structure. Like other members of the protein tyrosine kinase family, IGFRK-0P is composed of two domains connected by a single stretch of the polypeptide (the so-called hinge region from residue 1049 to residue 1055).

As shown in Fig. 2, the N-terminal domain is predominantly a twisted β-sheet containing five antiparallel β-strands ($\beta1$–$\beta5$). Flanking one side of the β-sheet is a single helix known in other tyrosine kinases as αC. The ordered segment of the N-terminus begins with residue Ser952. The C-terminal domain of the kinase comprises eight helices (αD, αE, αEF, αF–αJ) and four short β-strands ($\beta7$, $\beta8$, $\beta10$, $\beta11$). Lining the ATP-binding pocket of the IGFRK-0P and residing at the interface of the two domains are the hinge region (1049–1055), parts of the glycine-rich phosphate-binding loop between strands $\beta1$ and $\beta2$ (975–982), the catalytic loop (1103–1112) and the activation loop (1122–1144).

3.4. Dimer formation within an asymmetric unit

The two IGFRK-0P molecules within an asymmetric unit associate as a dimer in two possible ways, as shown in Fig. 3. In one, the active sites of the two monomers face each other, with each monomer contributing ~1 500 Å^2 (Fig. 3*a*) to the buried surface area. In the other, the active sites of the two monomers

face away from each other, with each monomer contributing ~800 Å^2 to the buried surface area (Fig. 3*b*). IGFRK-0P is known to exist as a monomer in solution. However, the fact that the intact IGF-1R receptor functions as a dimer allows speculation about the possible physiological role of the dimers observed in the present crystal form.

The dimer shown in Fig. 3(*a*) has been discussed previously (Munshi *et al.*, 2002). Using it as a model, one could visualize the *trans*-autoinhibitory role of the juxtamembrane region, accomplished by the ordered N-terminus of one monomer that approaches the active site of the other. However, in light of the recent structural and kinetic studies on the *cis*-autoinhibitory role of Tyr984 in the juxtamembrane of insulin receptor (Li *et al.*, 2003), autoinhibition of IGF-1R may be accomplished by Tyr957 (equivalent to Tyr984 of IR) in a similar fashion. Tyr957 in IGFRK-0P interacts with several other residues in the N-terminal lobe of the kinase domain, stabilizing a catalytically non-productive position of helix *αC* (Munshi *et al.*, 2002) and thus contributing to autoinhibition. In addition, it is not obvious from this model how the *trans*-autophosphorylation of IGF-1R receptor could be accomplished.

On the other hand, the dimer with the active sites facing away from each other (Fig. 3*b*), despite the lower buried surface area at the interface, appears to be consistent with the *cis*-autoinhibitory role of the juxtamembrane region of the receptor tyrosine kinases (Cann & Kohanski, 1997; Cann *et al.*, 1998; Li *et al.*, 2003). Moreover, intermolecular *trans*-autophosphorylation of the activation loop is conceivable since the active site and the activation loop of both monomers are now accessible.

3.5. Crystal packing

Fig. 4(*a*) shows that the dimers of the mutant IGFRK-0P are packed in layers perpendicular to the crystallographic dyad.

Molecules also pack as dimers in the crystals of wild-type IGFRK-0P (Munshi *et al.*, 2002). However, as shown in Fig. 4(*b*), the adjacent layers of the dimers stack differently between the wild-type and the mutant crystal forms. The molecular centroids of the dimers in the adjacent layers of the mutant crystal are shifted in the crystal *ac* plane, resulting in a 7 Å increase in unit-cell length along the *b* axis (b = 85.6 Å) compared with the wild type (b = 78.1 Å). Interactions between the dimer layers include parts of the protein proximal to the kinase insert region, suggesting that the E1067A and E1069A substitutions in the kinase-insert region facilitate different crystal-packing interactions.

Residues 1067–1072 of the kinase-insert region are disordered in the wild-type structure. Placing the mutant structure into the wild-type crystal packing arrangement reveals that the side chain of Glu1069 in the wild-type structure would be in close contact with the side chains of residues Glu1253 and Glu1254 of the neighboring molecule from the next layer of dimers. Charge repulsion among the side chains of these glutamate residues may contribute to the disorder of the kinase-insert region in the wild-type structure. Replacement of the larger polar side chain in glutamate with a smaller apolar side chain in alanine results in a different packing in the mutant crystals that maintains an ordered kinase-insert region. This observation is consistent with the idea that a reduced conformational entropy at the protein surface improves the odds of crystallizing a protein (Longenecker *et al.*, 2001).

3.6. Comparison of the wild-type and mutant IGFRK-0P structures

As expected, similarity in the structures of the mutant and the wild-type IGFRK-0P is conserved both at the monomer and the dimer levels. The C$^\alpha$ atoms of the two structures superimpose with a root-mean-square deviation of 0.3 Å. The conformations of both the N- and the C-terminal domains and their relative orientations are conserved between the two structures. However, the side-chain conformations of several surface residues differ between the two structures. In the wild-type structure, the N-terminal residues 944–951, residues of the kinase-insert region 1067–1072 and the C-terminal residues 1257–1264 are disordered. In the mutant IGFRK-0P structure, the first ordered residue at the N-terminus is 947. The C-terminal residues 1257–1264 are disordered in both the wild-type and mutant structures. In the mutant structure, the entire kinase-insert region is ordered. The tyrosine kinase domain of IGF-1R shares 84% sequence identity with the

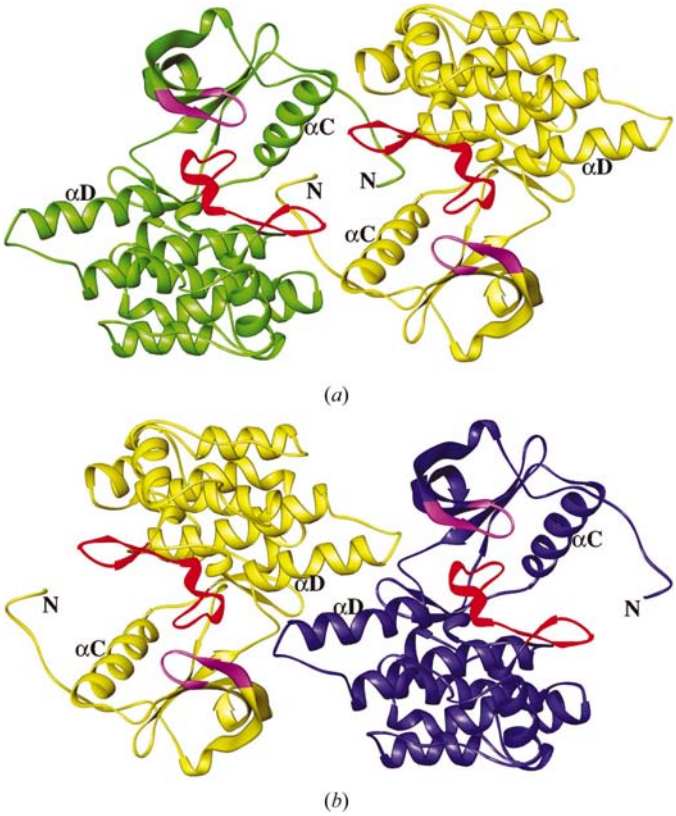

Figure 3
(*a*) IGFRK-0P dimer with active sites facing each other. The N-terminus of one molecule approaches the active site of the other. The P-loop is colored lavender and the activation loop is colored red. (*b*) IGFRK-0P dimer with active sites facing away from each other. The P-loop is colored lavender and the activation loop is colored red.

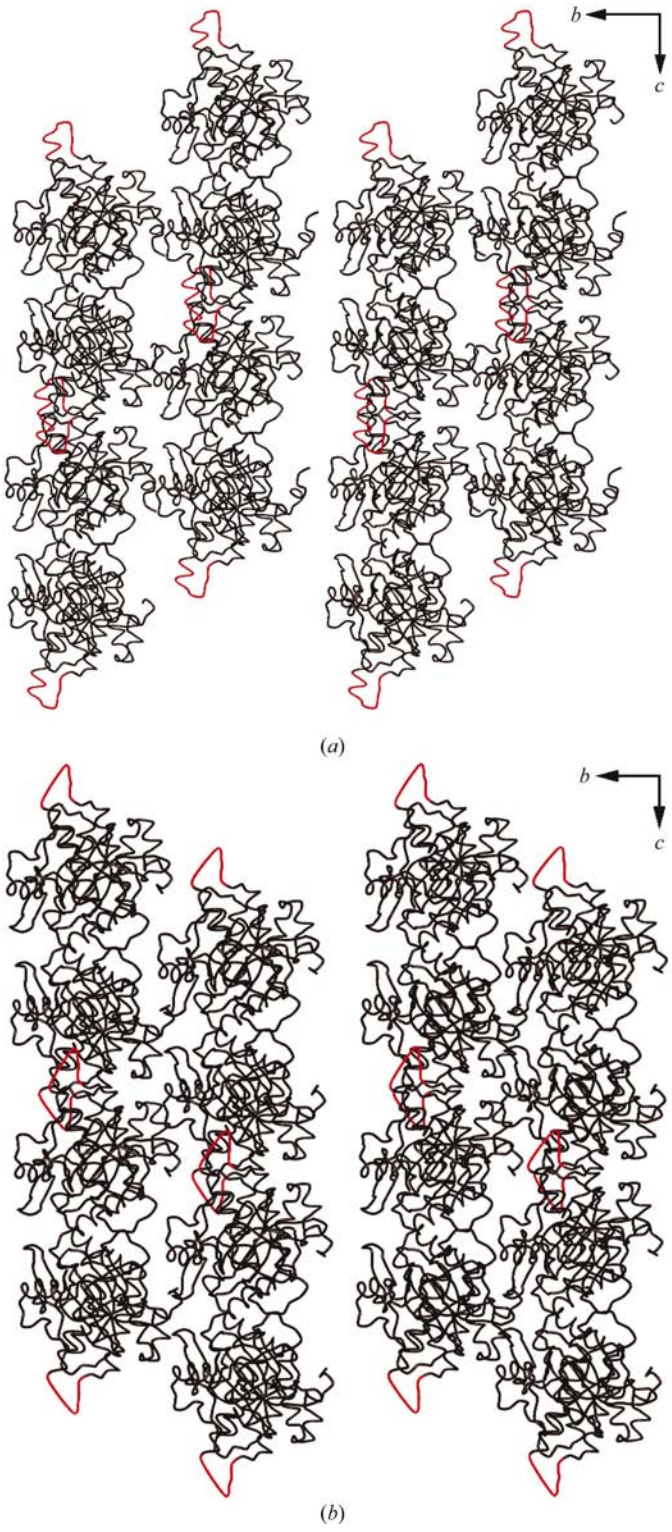

Figure 4
(*a*) Stereoview of the crystal packing of mutant IGFRK-0P in the *bc* plane. The kinase-insert region is highlighted in red. Association of dimers leads to layers of dimers perpendicular to the crystallographic *b* axis. (*b*) Stereoview of the crystal packing of wild-type IGFRK-0P in the *bc* plane. The disordered kinase-insert region, modeled as a loop, is highlighted in red. Association of dimers leads to layers of dimers perpendicular to the crystallographic *b* axis. The kinase-insert region from one layer of dimers is proximal to the ordered C-terminus from the adjacent layer of dimers.

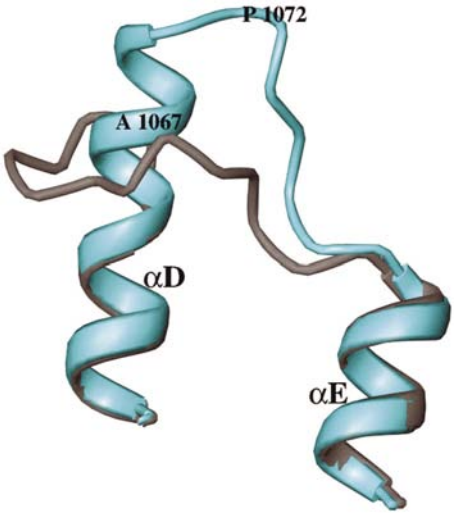

Figure 5
Superposition of the kinase-insert region (between the helices *D* and *E*) in IRK-0P (grey) and IGFRK-0P (cyan).

tyrosine kinase domain of insulin receptor (IRK) (Blakesley *et al.*, 1996; Ullrich *et al.*, 1986). Based on the comparison with the structure of unactivated kinase domain of the IRK (IRK-0P; Hubbard, 1994), the kinase-insert region of the wild-type IGFRK-0P structure has been suggested to adopt a conformation different from that observed in IRK-0P (Munshi *et al.*, 2002). The high-resolution IGFRK-0P structure affirms this suggestion, although two amino-acid substitutions have been incorporated.

Fig. 5 depicts a comparison of the conformation of the kinase-insert regions in IRK-0P and mutant IGRRK-0P. It is possible that the kinase-insert region is intrinsically mobile and that crystal-packing influences its eventual conformation. In addition, owing to the higher resolution of the mutant IGFRK-0P structure, a larger number of solvent molecules are well defined in the mutant structure compared with that of wild-type IGFRK-0P.

4. Conclusion

In summary, a 1.5 Å resolution structure of IGFRK-0P has been obtained by the use of a crystal prepared with a form of the enzyme that contains two surface point mutations. This structure resembles that determined for the wild-type IGFRK-0P at 2.7 Å resolution (Munshi *et al.*, 2002), with the exception of the kinase-insert region being ordered in the mutant structure. The ATP-binding pocket, the relative orientation of the N- and C-terminal lobes, the conformation of the activation loop and the catalytic residues are highly conserved between the mutant and wild-type structures.

We would like to thank the staff at the beamline 17-ID of IMCA-CAT for their help during data collection. The advanced Photon Source is supported by the US Department

of Energy, Basic Energy Sciences, Office of Energy Research under contract No. W-31-109-Eng-38.

References

Adams, T. E., Epa, V. C., Garrett, T. P. J. & Ward, C. W. (2000). *Cell. Mol. Life Sci.* **57**, 1050–1093.

Baserga, R. (1996). *Trends Biotechnol.* **14**, 150–152.

Baserga, R. (1999). *Exp. Cell. Res.* **253**, 1–6.

Baserga, R., Hongo, A., Rubini, M., Prisco, M. & Valentinis, B. (1997). *Biochim. Biophys. Acta*, **1332**, 105–126.

Baserga, R., Sell, C., Porcu, P. & Rubini, M. (1994). *Cell Prolif.* **27**, 63–71.

Bhatavdekar, J. M. & Neema, J. P. (1994). *Neoplasma*, **41**, 101–103.

Blakesley, V. A., Scrimgeour, A., Esposito, D. & LeRoith, D. (1996). *Cytokine Growth Factor Rev.* **7**, 153–159.

Brünger, A. T., Adams, P. D., Clore, G. M., Gros, P., Grosse-Kunstleve, R. W., Jiang, J.-S., Kuszewski, J., Nilges, M., Pannu, N. S., Read, R. J., Simonson, T. & Warren, G. L. (1998). *Acta Cryst.* D**54**, 905–921.

Cann, A. D., Bishop, S. M., Ablooglu, A. J. & Kohanski, R. A. (1998). *Biochemistry*, **37**, 11289–11300.

Cann, A. D. & Kohanski, R. A. (1997). *Biochemistry*, **36**, 7681–7689.

Collaborative Computational Project, Number 4 (1994). *Acta Cryst.* D**50**, 760–763.

D'Ambrosio, C., Ferber, A., Resnicoff, M. & Baserga, R. (1996). *Cancer Res.* **56**, 4013–4020.

Favelyukis, S., Till, J. H., Hubbard, S. R. & Miller, W. T. (2001). *Nature Struct. Biol.* **8**, 1058–1063.

Gansler, T. & Garvin, A. J. (1989). *Am. J. Pathol.* **135**, 961–966.

Garrett, T. P. J., McKern, N. M., Luo, M. Z., Frenkel, M. J., Bentley, J. D., Lovrecz, G. O., Elleman, T. C., Cosgrove, L. J. & Ward, C. W. (1998). *Nature (London)*, **394**, 395–399.

Hubbard, S. R. & Till, J. H. (2000). *Annu. Rev. Biochem.* **69**, 373–398.

Hubbard, S. R., Wei, L., Ellis, L. & Hendrickson, W. A. (1994). *Nature (London)*, **372**, 746–754.

Laskowski, R. A., MacArthur, M. W., Moss, D. S. & Thornton, J. M. (1993). *J. Appl. Cryst.* **26**, 283–291.

LeRoith, D., Werner, H., Beitner-Johnson, D. & Roberts, C. T. Jr (1995). *Endocr. Rev.* **16**, 143–163.

Li, S., Covino, N. D., Stein, E. G., Till, J. H. & Hubbard, S. R. (2003). In the press.

Longenecker, K. L., Garrard, S. M., Sheffield, P. J. & Derewenda, Z. S. (2001). *Acta Cryst.* D**57**, 679–688.

Macaulay, V. M., Everard, M. J., Teale, J. D., Trott, P. A., Van Wyk, J. J., Smith, I. E. & Millar, J. L. (1990). *Cancer Res.* **50**, 2511–2517.

Mercola, D. & Cohen, J. S. (1995). *Cancer Gene Ther.* **2**, 47–59.

Munshi, S., Kornienko, M., Hall, D., Reid, J., Waxman, L., Stirdivant, S., Darke, P. & Kuo, L. C. (2002). *J. Biol. Chem.* **277**, 38797–38802.

Navaza, J. (1994). *Acta Cryst.* A**50**, 157–163.

Oh, Y., Muller, H. L., Neely, E. K., Lamson, G. & Rosenfeld, R. G. (1993). *Growth Regul.* **3**, 113–123.

Otwinowski, Z. & Minor, W. (1997). *Methods Enzymol.* **276**, 307–326.

Pautsch, A., Zoephel, A., Ahorn, H., Spevak, W., Hauptman, R. & Nar, H. (2001). *Structure*, **9**, 955–965.

Prager, D., Li, H. L., Asa, S. & Melmed, S. (1994). *Proc. Natl Acad. Sci. USA*, **91**, 2181–2185.

Resnicoff, M. & Baserga, R. (1996). *J. Exp. Ther. Oncol.* **1**, 385–389.

Ullrich, A., Gray, A., Tam, A. W., Yang-Feng, T., Tsubokawa, M., Collins, C., Henzel, W., Le Bon, T., Kathuria, S. & Chen, E. (1986). *EMBO J.* **5**, 2503–2512.

Yarden, Y. & Ullrich, A. (1988). *Biochemistry*, **27**, 3113–3119.